Tapes of water hexamer clusters in the interlayer space of a 2D MOF: Structural, spectroscopic and computational insight of the confined water

ARTICLE *in* POLYHEDRON · JANUARY 2012

Impact Factor: 2.01 · DOI: 10.1016/j.poly.2011.10.030

7 AUTHORS, INCLUDING:

María C Bernini
Universidad Nacional de San Luis
17 PUBLICATIONS **187** CITATIONS
SEE PROFILE

Griselda E Narda
Universidad Nacional de San Luis
47 PUBLICATIONS **347** CITATIONS
SEE PROFILE

Alejandro Pedro Ayala
Universidade Federal do Ceará
188 PUBLICATIONS **1,523** CITATIONS
SEE PROFILE

Polyhedron xxx (2011) xxx–xxx

Contents lists available at SciVerse ScienceDirect

Polyhedron

journal homepage: www.elsevier.com/locate/poly

Tapes of water hexamer clusters in the interlayer space of a 2D MOF: Structural, spectroscopic and computational insight of the confined water

M.C. Bernini [a], E.V. Brusau [a], G.E. Narda [a,*], G. Echeverria [b,c], A. Fantoni [b], G. Punte [b], A.P. Ayala [d]

[a] INTEQUI, Departamento de Química, Facultad de Química, Bioquímica y Farmacia, Universidad Nacional de San Luis, 5700 San Luis, Argentina
[b] LANADI e IFLP, Departamento de Física, Facultad de Ciencias Exactas, 1900 La Plata, Argentina
[c] Facultad de Ingeniería, Universidad Nacional de La Plata, CC67, 1900 La Plata, Argentina
[d] Departamento de Física, Universidade Federal do Ceará, 60455-900 Fortaleza, CE, Brazil

ARTICLE INFO

Article history:
Received 9 July 2011
Accepted 28 October 2011
Available online xxxx

Keywords:
Er(III)-succinate
Water hexamers
Hydrogen bonds
Density functional calculations
MOFs

ABSTRACT

The synthesis, crystal structure and characterization of $[Er_2(C_4H_4O_4)_3(H_2O)_4]\cdot 6H_2O$, with particular emphasis on the structural details and the vibrational behavior of the highly organized sub-net of water are reported. X-ray structural analysis reveals that the hybrid framework, which can be classified as belonging to the I^0O^2 type, acts as a host of an infinite tape of six-membered water rings with distorted chair conformation. The water network extends between the hybrid layers helping the close packing and the stabilization of the structure through H-bond interactions, with further development of the supramolecular tridimensional structure. The self-assembly of the hydration water molecules is conditioned by the hybrid host, forcing them to adopt a less stable conformation when compared with hexagonal ice. The vibrational spectra of partially and completely dehydrated samples as well as of partially isotopic diluted ones have been obtained and analyzed. In order to guide the assignment of the vibrational spectra a theoretical calculation was performed at the B3LYP/6-31G** level for a model consisting of three water clusters.

1. Introduction

Hydrogen bonding involving water molecules together with other non-covalent interactions are capable of guiding the self-assembly processes in chemical systems [1]. In turn, hydrogen bond (HB) interactions and their fluctuations determine the properties of bulk water. The lack of a correct evaluation of these interactions has been the major impediment to understand the "anomalous" behavior of water [2]. The apparently simple water molecule develops one of the more complex condensed phases, a fact that promotes a considerable effort devoted to theoretical and experimental investigations on all forms of water, including free and confined clusters, bulk water and ice polymorphs [3].

Structural chemistry of water is comparable with that of a sp^3-carbon atom, because in both cases there are four possible binding sites. However, the larger flexibility of HB geometries allows the topologies of water clusters to depart from the ideal minimum energy conformations. The six-membered rings are the preferred configuration of water clusters, probably due to the saturation of the HB cooperative effects [4], and several almost isoenergetic low-lying structural isomers exist, viz. cage, prism, book, boat, and other cyclic conformations according to theoretical calculations [5,6]. However, the lattice of a crystal host may offer an appropriate environment for stabilizing a higher energy hexamer topology. Thus, several clusters in chair conformation have been identified in host lattices [7].

Guess water molecules are often crystallographically disordered and they merely play a space filling role when there are cavities of suitable size [7a]. A rather different situation is found in porous coordination polymers (PCP) that, as inorganic zeolites, usually crystallize with solvent confined inside the pores or channels. It is in fact widely accepted that in these systems solvent-framework as well as solvent–solvent interactions are important as regards the stability and the specific features of the resulting crystal framework [8,9]. Therefore, the study of enclathrated water is important to understand the formation mechanism of different metal-organic frameworks (MOFs). Although the role of water clusters and their structure have not been properly highlighted in the structural study of hybrid compounds in the past, the organization level that water adopts through HB interactions when confined in the channels of such compounds is currently a matter of growing interest [10].

Clusters of different size and water molecules connectivity have been found in MOFs or extended inorganic hybrids. Some examples with increasing complexity in their motifs would be: isolated dimers and hexamers in Ce(III)- and Pr(III)-pyridine-2,6-dicarboxylate frameworks [2]; tapes of hexamers in a metal phosphonocarboxylate

* Corresponding author.
E-mail address: gnarda@unsl.edu.ar (G.E. Narda).

0277-5387/$ - see front matter © 2011 Elsevier Ltd. All rights reserved.
doi:10.1016/j.poly.2011.10.030

network [11]; 1D-chains of fused pentamers and hexamers in a compound based on Cu(II) and isophthalate [12]; 1D-chains of alternating four-members and six-members clusters in a zinc(II)-pyridine-2,5-dicarboxylate complex [13]; a tape structure featuring vertex-sharing cyclic hexamers hosted within the $[Fe(bipy)_2(CN)_2]\cdot 2.5H_2O$ complex [14]; a 2-D water structure based on cyclic hexamers and decamers in a MOF built from Er(III) and fumaric acid [9]; hybrid water–organic layers in a Cu(II) coordination polymer [15] where three types of isolated water clusters ($(H_2O)_6$, $(H_2O)_8$, and $(H_2O)_{10}$) build up H-bonded layers with benzenedicarboxylate anions; and a 2D arrangement of water tetramers and octamers and phthalic acid in $[Cd_2(phen)_4(p\text{-}phth)(H_2O)_2]\text{-}(p\text{-}phth)\cdot 10H_2O$ [16].

In spite of the crucial structural role of water molecules that link the hybrid layers allowing the tridimensional development of the solid, the vibrational behavior of their highly organized sub-network has only received marginal attention, and no systematic data is found in the literature.

Here we report a detailed structural description of a water hexamer tape developed in the interlayer space of an erbium hybrid framework belonging to an isostructural series of lanthanide succinates – $[Ln_2(C_4H_4O_4)_3(H_2O)_4]\cdot 6H_2O$ (Ln = Dy-Yb) – obtained at room temperature. Appropriate experimental and theoretical methods have been used to investigate the vibrational properties of such a highly organized water system. Seeking for a complete and reliable assignment of the vibrational spectra, we have compared the spectra of partially and completely dehydrated samples as well as of partially isotopic diluted ones. To improve the assignment, the association of IR-Raman bands with specific water molecules has also been supported by theoretical calculations of the vibrational spectrum of a proposed model of fused water hexamers.

2. Experimental

2.1. Synthesis of $[Er_2(C_4H_4O_4)_3(H_2O)_4]\cdot 6H_2O$

Reagents of analytical grade were used in the synthesis. $ErCl_3\cdot 6H_2O$ (2 mmol) was dissolved in distilled water (100 mL) and then added to an aqueous solution containing succinic acid (3 mmol, 100 mL) with permanent stirring. The resulting pH was raised to 4.5 by adding KOH. The solution was allowed to evaporate slowly at room temperature. A large number of pink needle-shaped single crystals suitable for a crystallographic study was obtained after several days. These were filtered, washed with distilled water, and dried at room temperature. Yield: 70%. Elemental *Anal.* Calc.: C, 16.69; H, 3.71. Found: C, 16.53; H, 3.59%. Thermal analysis results, including TG–DTA curves, are displayed in Fig. S1 (see Supplementary data).

2.2. Isotopic dilution procedure

Twenty milligrams of the erbium compound described above were suspended in D_2O (5 mL, Merck 99.9%) under stirring conditions for 1 day at room temperature. Finally, the sample was dried by evaporation of the solvent in vacuum at 50 °C. The degree of deuteration achieved was estimated to be 50%.

2.3. Single-crystal structure determination

Crystal data were collected on an automatic four-circle CAD-4 diffractometer at room temperature (293 K). CAD-4 software was used for data collection and cell refinement [17]. The program XCAD-4 [18] was employed for data reduction. The structure was solved by direct methods using SHELXS-86 [19] and refined by full-matrix least-squares based on F^2 using SHELXL-93 [20]. The succinate hydrogen atoms in both structures were located from a difference-Fourier synthesis, while the program CALC-OH [21] was used to calculate the position of the hydrogen atoms of water. Further refinements were performed with the hydrogen atoms riding on bound atoms. The structural analyses were performed with PLATON [22] and PARST [23]. The molecular graphics were produced with ORTEP [24]. Crystal data and details of data collection and structure refinement are given in Table 1. Atom labeling is shown in Fig. 1. Selected interatomic distances and bond and torsion angles are listed in Table 2. HB geometries are reported in Table 3.

Comparison of the experimental PXRD pattern (see Fig. S2) with the simulated one obtained from the single-crystal XRD data confirms that the structural elucidation is representative of the bulk material.

2.4. Infrared and Raman spectroscopy

FTIR spectrum at room temperature was recorded using the KBr pellet technique. The spectra at controlled increasing temperatures were recorded placing the pellet in a variable-temperature IR cell in the range 25–270 °C. The spectrum of the partially deuterated sample was recorded using CsI windows and dispersed in mineral oil (Nujol). A Nicolet Protégé 460 spectrometer working in the 4000–225 cm^{-1} range with 32 scans and with 4 cm^{-1} of spectral resolution was employed in all cases. Raman spectra were recorded with a Jobin-Yvon T64000 triplemate spectrometer using the lines 514.5 nm (Ar+ ion laser) and 532 nm (solid state laser) in order to exclude the erbium luminescent emission. The slit widths were adjusted to yield a 2 cm^{-1} resolution. A liquid N_2 – cooled CCD detector was used.

Table 1
Crystal data, structure determination and refinement summary for $[Er_2(C_4H_4O_4)_3(H_2O)_4]\cdot 6H_2O$.

Crystal information	
Crystal system	triclinic
Chemical formula	$C_6H_{16}ErO_{11}$
Formula weight	431.45
Space group	$P\bar{1}$
a (Å)	6.5230(13)
b (Å)	9.7807(12)
c (Å)	10.4712(5)
α (°)	80.215(6)
β (°)	89.872(8)
γ (°)	71.376(12)
V (Å^3)	622.90(15)
ρ_{calc} (g cm^{-3})	2.300
Z	2
$F(000)$	416
μ [Cu Kα] (mm^{-1})	13.034
Crystal size	0.26 × 0.12 × 0.04
T_{min}/T_{max}	0.1327/0.6237
Data collection	
Temperature (K)	293(2)
λ [Cu Kα] (Å)	1.54184
Monochromator	graphite
θ range for data collection	4.29–69.90
Completeness to θ	99.2%
Limiting indices	$-7 \leqslant h \leqslant 1$ $-11 \leqslant k \leqslant 11$ $-12 \leqslant l \leqslant 12$
Structure refinement	
Reflections collected/unique with $I > 2\sigma(I)$	2959/2316 (R_{int} = 0.0394)
Refined parameters	164
Goodness-of-fit on F^2	1.103
R	0.0466
R_w	0.1334
$(\Delta/\rho)_{max}/(\Delta/\rho)_{min}$ (e Å^{-3})	1.736/−2.142

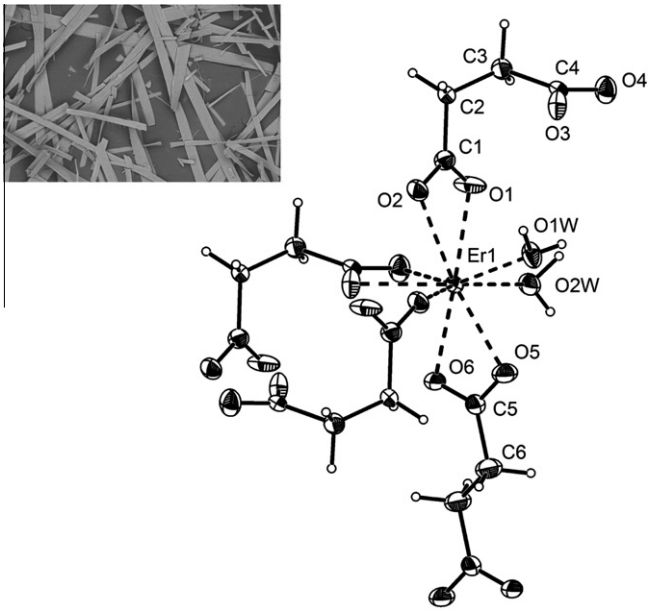

Fig. 1. ORTEP-III view of the coordination polyhedron of Er(III) showing the atom-labeling scheme. Displacement ellipsoids are drawn at 50% probability. Inset: SEM image of the crystal habit of $[Er_2(C_4H_4O_4)_3(H_2O)_4]\cdot 6H_2O$.

2.5. Computational methods

As a first approximation, the vibrational modes involving water molecules hosted in the crystal were estimated using a very simplified model system. It consists of 10 and 4 water molecules representative of the hydration and coordination types, respectively. Since hydrogen atom positions are very poorly determined from X-ray diffraction data, a partial geometry optimization of the hydrogen atom internal coordinates was performed, keeping the relative positions of oxygen atoms as in the crystal. This approximation was aimed to preserve the water cluster conformation induced by the crystal environment. The resulting hydrogen atom positions are consistent with a very stabilizing HB set. Vibrational frequencies were calculated for the resulting structure. Calculations were performed with GAUSSIAN 98/03 set of programs [25,26], using the density functional theory (DFT) with the hybrid Becke's three-parameters exchange functional (B3) [27] in combination with the Lee–Yang–Parr correlation functional (B3LYP) [28]. The split-valence basis set 6-31G** and standard convergence criteria for both SCF and geometry optimization were used. Calculated frequency values scaled by 0.96 were used in the analysis.

Table 3
Non-hydrogen atoms short contacts geometry[a] in $[Er_2(C_4H_4O_4)_3(H_2O)_4]\cdot 6H_2O$ (distances: Å, angles: °, e.s.d's in parentheses).

Distances (Å)		Angles (°)	
O1W···O6	2.797(7)	O3W···O2W···O5W	99.0(2)
O1W···O3[v]	2.660(6)	O2W···O3W···O5W	129.0(3)
O2W···O3W	2.735(8)	O2W···O5W···O3W	77.6(2)
O2W···O5W	2.694(7)	O5W···O4W···O3W	104.6(3)
O3W···O4W	2.93(1)	O4W···O3W[vi]···O5W	100.4(3)
O5W···O3W[vi]	2.838(8)	O3W···O5W···O4W[ii]	82.4(2)
O5W··· O4W[ii]	2.73(1)		
O3W···O4	3.060(8)		
O3W···O6	3.096(8)		
O4W···O6	2.970(8)		
O5W···O5[v]	2.736(8)		
C6–H61···O4W[vii]	3.53(1)		

Symmetry codes: [v] $-x+1, -y-1, -z$; [vi] $-x, -y, -z-1$; [vii] $1-x, -1-y, -z$.
[a] Water hydrogens are omitted due to detected waters disorder.

3. Results and discussion

3.1. Structure description of the hybrid framework

Single-crystal X-ray diffraction data presented here for $[Er_2(C_4H_4O_4)_3(H_2O)_4]\cdot 6H_2O$ (**1**) indicates that it is isostructural with the compound obtained by hydrothermal synthesis [29] and also with the $[Ho_2(C_4H_4O_4)_3(H_2O)_4]\cdot 6H_2O$ reported by us [30].

Compound **1** crystallizes in the triclinic space group $P\bar{1}$ with $Z=2$ and the following cell parameters: $a=6.5230(13)$ Å, $b=9.7807(12)$ Å, $c=10.4712(5)$ Å, $\alpha=80.215(6)°$, $\beta=89.872(8)°$ and $\gamma=71.376(12)°$; cell volume is 622.90(16) Å^3.

A brief description of the hybrid framework is presented below and includes interesting information not given in Refs. [29,30]. There are two crystallographically independent succinate anions. One of them, located on an inversion center, has a perfect *trans* conformation (torsion angle: 180°), the other one having a *gauche* conformation with a torsion angle of 61.8(7)°. Both carboxylate groups of the *trans* and *gauche* isomers bind in a chelating mode. Additionally, one O atom of the *gauche* anion also acts in a bridging mode.

The Er(III) cations are coordinated by nine oxygen atoms, seven of them belonging to four succinate anions and the others to two crystallographically inequivalent water molecules, as shown in Fig. 1. Edge-sharing polyhedra, related by an inversion center form centrosymmetric dimers where the Er(III) cations are connected by two chelating bridging carboxylates, with the chelating plane (CP) departing 13.2(4)° from the bridging plane (BP) (see Table 2). These dimers are further strengthened by a HB interaction involving

Table 2
Selected intramolecular bond distances (Å), bond angles (°) and torsion angles (°) for $[Er_2(C_4H_4O_4)_3(H_2O)_4]\cdot 6H_2O$.

Er1–O1W	2.349(4)	C1–O2	1.271(8)	Er1–O2–Er1[i]	112.97(16)
Er1–O2W	2.315(4)	C1–C2	1.500(9)	O1–C1–C2–C3	−27.6(9)
Er1–O1	2.384(4)	C2–C3	1.527(8)	O2–C1–C2–C3	152.2(6)
Er1–O2	2.600(5)	C3–C4	1.519(8)	C1–C2–C3–C4	−62.0(7)
Er1–O2[i]	2.321(4)	C4–O3	1.270(8)	C2–C3–C4–O3	−26.1(8)
Er1–O3[ii]	2.374(4)	C4–O4	1.247(7)	C2–C3–C4–O4	154.9(6)
Er1–O4[iii]	2.485(5)	C5–O5	1.258(8)	O5–C5–C6–C6[iii]	−172.2(8)
Er1–O5	2.390(4)	C5–O6	1.259(8)	O6–C5–C6–C6[iii]	8.9(13)
Er1–O6	2.448(4)	C5–C6	1.501(9)	C5–C6–C6[iv]–C5[iv]	180.0(1)
C1–O1	1.237(8)	C6–C6[iii]	1.499(14)		
Plane P1: atoms:		*Plane P2: atoms:*		*Plane P3: atoms:*	
Er1 O2 Er1[i] O2[i][i]		Er1 O1 O2		Er1 O1w O3[ii] Er1[i]	
<P1,P2> = 13.2(4)°		<P2,P3> = 89.8(2)°			

Symmetry codes: [i] $-x, -1-y, -z$; [ii] $1-x, -1-y, -z$; [iii] $-1+x, y, z$; [iv] $x+1, y, z$.

coordinated water W1 and the carboxylate oxygen O3. Er dimers can be seen as zero-dimensional secondary building units (SBUs). Therefore, the resulting network can be classified as belonging to the I^0O^2 type according to Cheetham et al. [31].

The overall structure is described as 2D organic–inorganic polymeric layers parallel to the *ac* plane, as can be seen in Fig. 2a. Within layers, dimers are connected by *gauche* succinate ligands along [1 0 0] and *trans* succinate ligands along [1 0 1]. The connection along [1 0 0] is further stabilized by a HB between W1 and the succinate oxygen O6. Er–O distances range between 2.315(4) and 2.600(5) Å, Er···Er distance within dimers is 4.1062(5) Å.

The hybrid framework acts as a host with channels that contain hydration water molecules related by inversion centers located at (n, 0, ½) with n integer. Water molecules form six-member clusters through HB interactions. The channels, parallel to *a* direction, occupy 25% (155.8 $Å^3$) of the total cell volume and develop between layers (see Fig. 3).

The coordinated water molecule W2 occupies a key position in the structure since it is oriented towards the channel, being in contact with the solvent molecules located in the interlayer space and helping in the formation of an infinite tape of six-membered rings as described in the next section.

Hydration water molecules are also hydrogen bonded to succinate anions, thus providing the connection between layers and the stabilization of the three-dimensional arrangement.

In order to get a better description of the structure of the 2D-coordination polymer a topological analysis of the covalent layers of the MOF has been performed using the TOPOS program [32]. The standard simplification method gave a bi-nodal net consisting of 3-connected nodes located on the *gauche* succinate anion and 4-connected nodes placed on the Er(III) ions. In this depiction the *trans* succinate ligand acts just as a linker and is represented as an edge in the Fig. 2b and c. The Point (Schläfli) symbol for the net is $\{4^2.6^3.8\}\{4^2.6\}$ and the corresponding topological type V_2O_5. However, the structure can be more simply described considering both succinate anions just as linkers that join 4-connected nodes located at the centroid positions inside the Er dimers. In this simpler representation a uni-nodal net is obtained, the Point (Schläfli) symbol for the net being $\{4^4.6^2\}$ and the topological type being sql-Shubnikov tetragonal plane net (see Fig. 2d and e).

3.2. Structural description of the H-bond interactions in the water tape

The three crystallographically independent hydration water molecules present in the asymmetric unit of **1** are linked by HBs to each other and also to three equivalent water molecules related by an inversion center. Thus, a six-membered cyclic cluster with chair conformation, called from now on as "Type A", is built up. Two equivalent coordination water molecules W2 related by an inversion center connect the clusters in the [1 0 0] direction, conforming other six-membered ring that includes two hydration water molecules (W3 and W5) and their corresponding centrosymmetric images. This cluster, termed "Type B", has also a chair conformation and shares the W3–W5 edge with the type A cluster (see Fig. 4).

According to Infantes and Motherwell [8], 81% of the isolated water hexamers in organic crystal lattices adopts the chair conformation. Additionally, one of the three more frequent tape-patterns consists of six-membered rings in chair conformation fused by sharing edges, which is denoted as T6(2), as described above.

The infinite H-bonded tape of water hexamers found in $[Er_2(C_4H_4O_4)_3(H_2O)_4]\cdot 6H_2O$ extends along the *a* direction, being therefore parallel to the shortest cell axis. This behavior is consistent with the empirical rule stated in Ref. [8] that correlates the direction of propagation of the chains, tapes and layers of encapsulated water with the short axis of the unit cell. This fact is associated with an increase in stability as the packing becomes denser. As can be seen from Fig. 3, the water tape is confined into the inter-lamellar space linking the hybrid layers as a "glue" and helping the close packing structure stabilization.

According to Kitagawa and co-worker review [33] on the relationship between the pores and guest molecules, template effects in PCPs can be divided in two types: Templating For Guests (TFG) and Templating By Guests (TBG). When molecules are located in nanospaces their properties are different from those of the corresponding bulk fluids. Such phenomenon is known as the stabilization effect of micropores and it enables the formation of an ordered phase of small molecules and/or provides a specific reaction nanoflask. In these cases, the PCP can be considered as a TFG. In the present framework, the average O···O distances within clusters Type A and B are 2.834(9) and 2.756(8) Å, respectively. The corresponding average values for O···O···O angles are 95.8(3) (Type A)

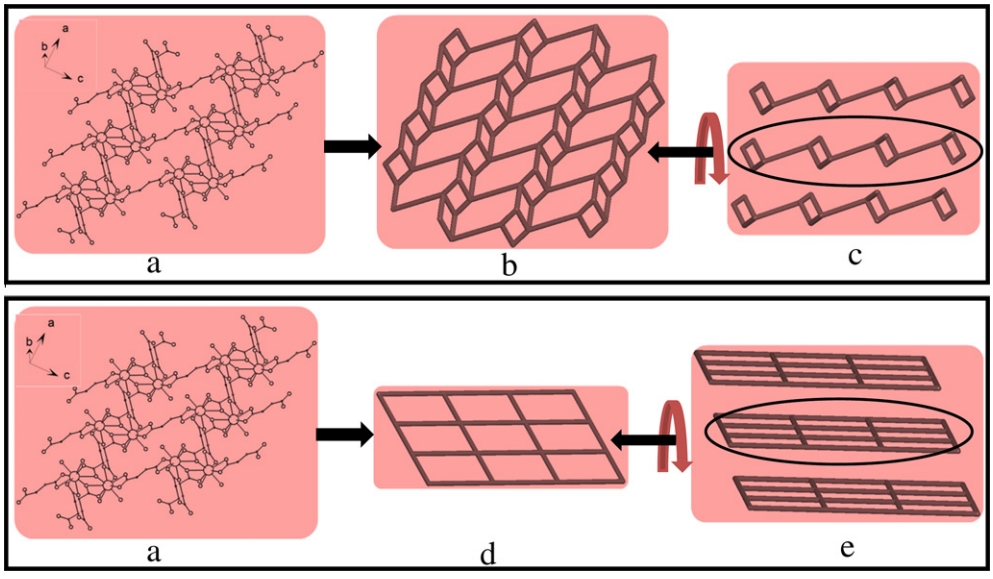

Fig. 2. (a) Projection of crystal structure along the b direction, (b) the same projection of the simplified network showing the 3- and 4-connected nodes, (c) representation of the layers crystal packing in the simplified net, (d) and (e) projections correspond to the simpler topological description.

Please cite this article in press as: M.C. Bernini et al., Polyhedron (2011), doi:10.1016/j.poly.2011.10.030

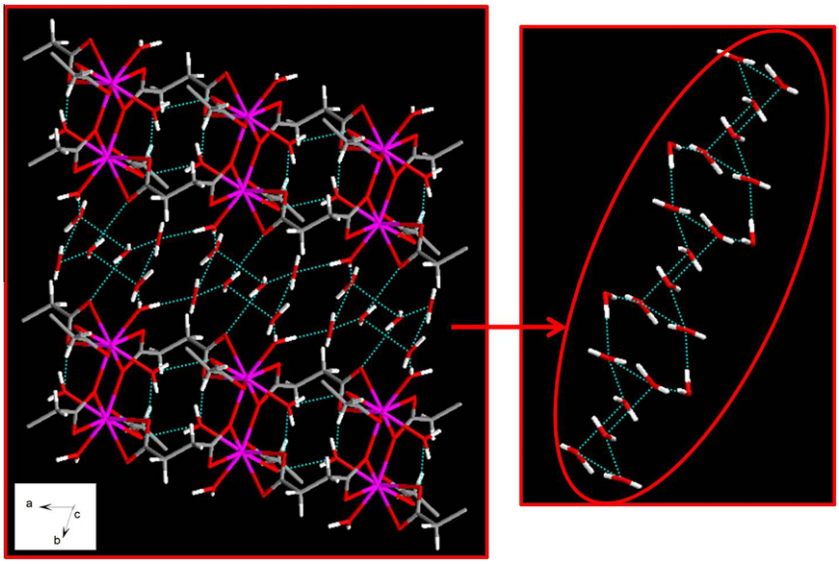

Fig. 3. Crystal packing showing hexamer clusters tapes linking the 2D-metal organic framework (left) and detail of the water hexamer tape (right).

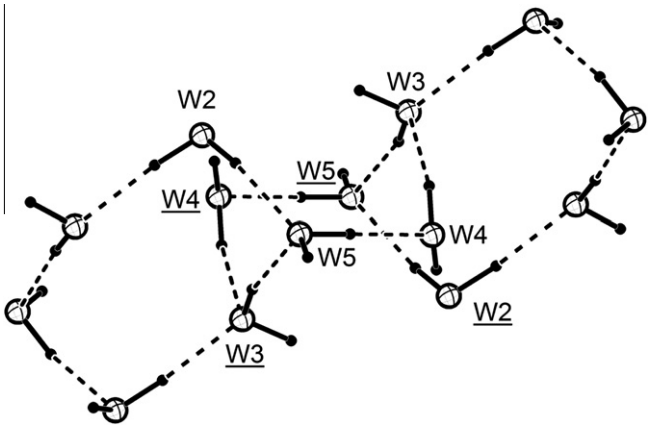

Fig. 4. Centro-symmetric model cluster employed for frequency calculations. Hydration water molecules: W3, W4, W5; coordination water molecule: W2.

and 101.9(3)° (Type B). The average O···O distance in A hexamer and average angle values in both hexamers deviate considerably from the respective geometric parameters found in hexagonal ice (2.759 Å and 109.3°) [34], thus reflecting the strong influence of the crystalline environment on the conformation exhibited by the rings. This fact accounts for the stabilization effect of micropores associated with the TFG function of the metal-organic framework [33]. The self-assembly of hydration water molecules is conditioned by the shape of the hybrid-host channels forcing them to adopt a less stable conformation when compared with hexagonal ice. This effect is more marked in ring A, whose geometrical features are closer to those of liquid water (e.g. average O···O distances 2.84 Å) [35]. A similar geometric situation was found by Wu and co-workers [36] in a 2D lamellar water network with metal-organic units acting as templates. According to those authors, in such a crystal the role of water clusters is shifted from being the guest to being the host, and the structure is stabilized through metal -organic guest inclusion. In the present case, the water tape plays an important role in the structural stabilization of the framework, providing the appropriate HB acceptors and donors necessary to maintain the linkage between hybrid layers with further development of the supramolecular tridimensional structure. In fact, the removal of hydration water by thermal treatment leads to an amorphous solid, as it has been observed for the isostructural holmium succinate hydrate [30].

Points of linkage between the water tape and the hybrid framework are found in the HB interactions exhibited by W3, W4 and W5 as donors and the carboxylate groups as acceptors, as well as in the weak interaction between W4 and a methylene group (see Table 3). However, the known limitation of X-ray data to locate protons, in addition to the disorder commonly found in ice structure, prevent us from ruling out other points of linkage. Because of that, a unique pattern of HB interactions can hardly be characterized only from a crystal structure determination. Moreover, several interaction patterns leading to similar interaction energies could be expected from the IR water bands broadening discussed below.

3.3. Experimental and theoretical vibrational characterization of the water clusters

The FTIR and Raman spectra of compound **1** are depicted in Fig. 5. Variable-temperature FTIR (VT-FTIR) spectra are gathered in Fig. 6 and the spectrum of the partially deuterated compound is shown in Fig. 7.

The selection of the bands that can be assigned to vibrational modes of water molecules was performed on the basis of their thermal and isotopic behavior and supported by the results obtained from theoretical calculation on a model system (see Section 2.5 and Fig. 4). Data reported for closely related systems were also taken into account [37]. The observed IR and Raman frequencies and their calculated counterparts are collected in Table 4.

3.4. Water stretching modes

The dehydration performed by VT-FTIR shows a progressive disappearance of the band at 3560 cm^{-1} revealing a component at higher frequency (about 3600 cm^{-1}) in the spectra of partially dehydrated samples. This band can be associated with the 3524 cm^{-1} calculated value, which corresponds to a stretching mode with dominant participation of W4 hydration water molecule. Moreover, calculation predicts a band located at 3612 cm^{-1} associated to W2 coordination water molecule.

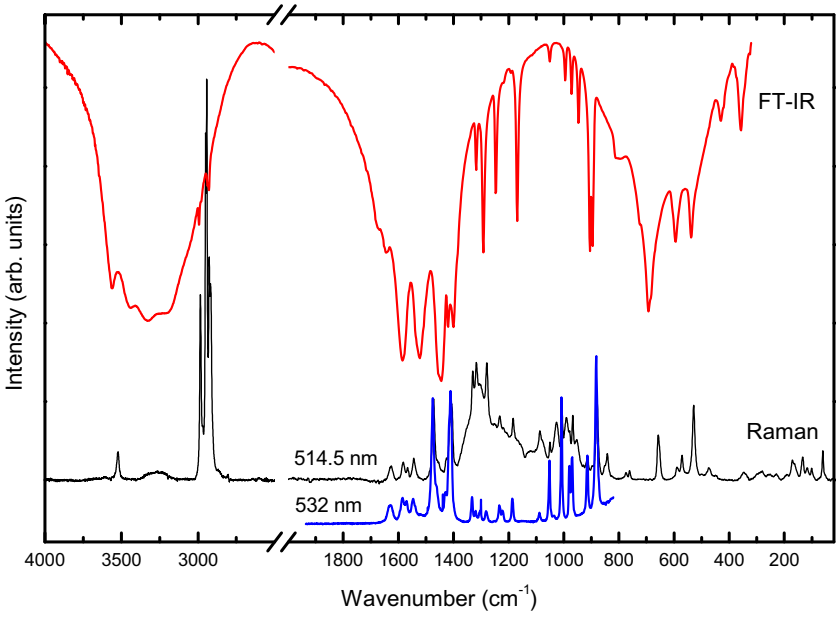

Fig. 5. FTIR (top) and Raman (bottom) spectra of $[Er_2(C_4H_4O_4)_3(H_2O)_4]\cdot 6H_2O$.

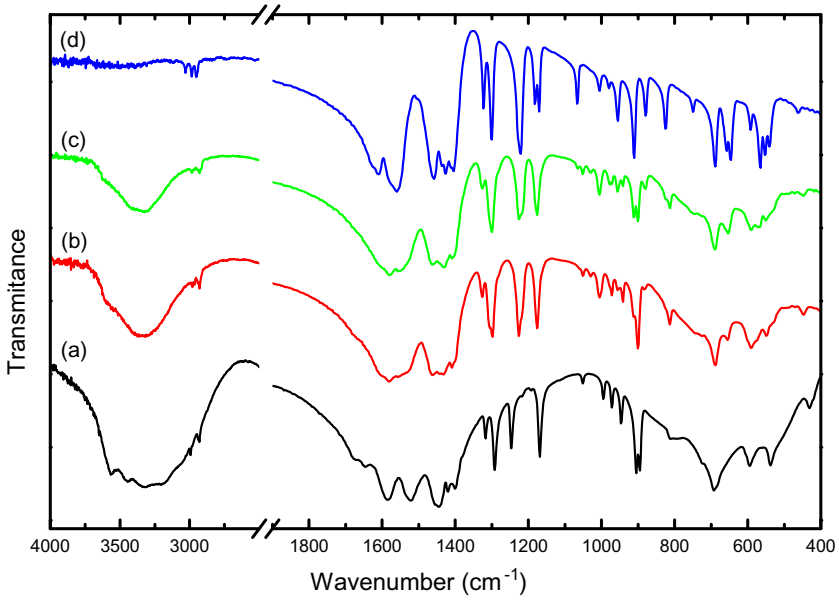

Fig. 6. Variable temperature FTIR spectra of $[Er_2(C_4H_4O_4)_3(H_2O)_4]\cdot 6H_2O$ from RT up to 250 °C.

The band at 3443 cm^{-1} which disappears when temperature rises can be associated with a calculated band at 3494 cm^{-1} coming from the stretching vibration of W4 hydration water molecule.

The most intense band in this zone is centered at 3323 cm^{-1}. Its intensity decreases gradually during heating, but it is the only band that remains up to almost total dehydration. On this basis, we assume that hydration and coordination water molecules vibrations contribute to such a band. Accordingly, theoretical calculation predicts a band at 3371 cm^{-1} with main contribution of a stretching mode that involves W2 as well as W3 water molecules. It is important to highlight that this observed frequency value is very close to that reported by Nauta and Miller for water hexamers with cyclic geometry obtained in liquid helium (3335 cm^{-1}) [38]; the difference between both experimental values being perfectly attributable to the differences between the geometries of the hexamers.

The lowest frequency value for the O–H stretching modes is located at 3170 cm^{-1}; the position of this component and its immediate modification under thermal treatment allow us to assign it to the W5 hydration water molecule, which, as already discussed, appears as one of the more structurally involved water molecules (see Table 3). Consistently, calculation shows a band at 3191 cm^{-1} which mainly derives from the stretching mode of that hydration water molecule.

The spectrum of the partially deuterated compound shows a broad and relatively strong band at 3260 cm^{-1} that can be satisfactorily associated with that at 2430 cm^{-1} in the O–D stretching zone. The corresponding νOH/νOD ratio (1.341) is in good agreement with the correlation νOH/νOD versus νOH of Berglund et al. for the HOD species [39]. The existence of D_2O species is evidenced by a band at 2380 cm^{-1} assigned to the O–D vibration.

Please cite this article in press as: M.C. Bernini et al., Polyhedron (2011), doi:10.1016/j.poly.2011.10.030

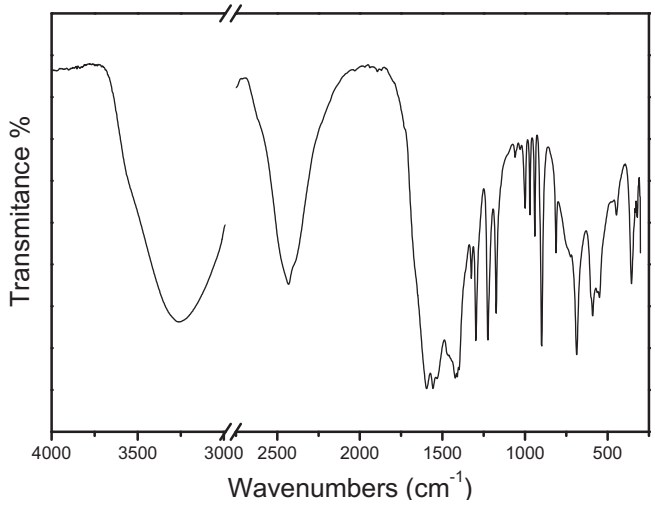

Fig. 7. FTIR spectrum of partially deuterated $[Er_2(C_4H_4O_4)_3(H_2O)_4]\cdot 6H_2O$.

3.5. Water deformation modes

Statistical studies of hydrated solids [40] demonstrated that deformation modes are usually present in a narrow range of frequencies. That is, 1582–1721 cm^{-1} (mean value, 1636 cm^{-1}) for H_2O, 1402–1470 cm^{-1} (mean value, 1426 cm^{-1}) for the HOD species, whereas the range extends from 1171 to 1248 cm^{-1} (mean value, 1194 cm^{-1}) for D_2O molecules. On the other hand, bending modes are sensitive to hydrogen bonding and coordination, that cause increase or decrease in their vibrational energy, respectively; the dynamic coupling of deformation modes derived from neighboring water molecules should also be considered [40].

The band at 1673 cm^{-1}, absent in the spectra of partially dehydrated samples, can be identified with a bending mode involving mainly W4, with a calculated frequency of 1676 cm^{-1}. The behavior of the medium intensity band at 1645 cm^{-1} with progressive heating is difficult to evaluate since this procedure also provokes widening and shifting to higher frequencies of the OCO antisymmetric stretching vibrations of the ligand, with the consequent overlapping of the signals. On the basis of the good coincidence with the calculated frequency (1655 cm^{-1}), it can be assigned to a deformation mode with similar contributions from coordination and hydration water molecules.

Additional spectroscopic evidence of these modes is found in the spectrum shown in Fig. 7. Two bands of notorious intensity at 1410 and 1227 cm^{-1} that appear on deuteration can in fact be related to HOD and D_2O deformation modes, respectively.

3.6. Water librational modes

The comparison among the spectra of partially and completely dehydrated samples was particularly useful to identify the librational modes of water molecules that appear below 1000 cm^{-1}. These modes are usually difficult to assign due to their low intensity and the occurrence in the same spectral zone and with similar features, of modes derived from methylene or carboxylate groups. Since these later bands can also be modified with increasing temperature, the analysis of the Raman spectrum and the exploration of the IR spectrum containing water molecules with an

Table 4
Assigment of water modes in the vibrational spectrum of $[Er_2(C_4H_4O_4)_3(H_2O)_4]\cdot 6H_2O$.

Observed IR freq.[a]	Observed Raman freq.	Calculated freq.[a,d] IR (Raman)	IR intensity[b,d]/Raman activity[c,d]	Observed IR freq. in the deuterated compound[a]	Assignment[e]
Stretching modes					
3600 (sh)		3612	947		νOH W2
3560 (s)	3516	3524(3519)	773/135		νOH W4
				3260 (m)	νOH HOD
3443 (s)		3494	332		νOH W4
3323 (s)		3371	1121		νOH [W2, W3]
					νOH W1
3170 (s)	3270	3191(3173)	2019/386		νOH W5
				2430 (m)	νOD HOD
				2380 (sh)	νOD D_2O
Deformation					
				1410 (s)	δHOD
1673 (sh)	1626	1676 (1672)	251/10		δW4
1645 (m)		1655	132		δ[W2, W3, W4, W1]
				1227 (m)	δD_2O
Twisting + rocking + wagging					
1247(m)					$\rho_t CH_2$
947 (s)		924	321		$(\rho_t + \rho_w)$W5, ρ_tW4
895 (m)		913	24		$(\rho_t + \rho_w)$W5, ρ_tW4
812 (sh)	839	850 (828)	170/3		ρ_wW4, $(\rho_t + \rho_w)$W2
790 (br,sh)		793	337		$(\rho_t + \rho_w)$W3
725 (sh)	759	746	859		$(\rho_t + \rho_w)$W2
720		726(722)	410/7		ρ_wW4
				560 (w)	ρ_t D_2O
537 (m)	530	569(569)	99/8		ρ_r[W2,W3]
				446 (w)	ρ_r HOD
430	471	431(447)	106/8		ρ_r[W5,W2,W4], ρ_tW3
358	349	358(358)	46/4		ρ_r[W5,W3,W2], ρ_tW4

s, strong; sh, shoulder; m, media; w, weak; ν, stretching; δ, deformation; ρ_r, rocking; ρ_w, wagging; ρ_t, twisting.

[a] Frequencies in cm^{-1}.

[b] IR intensity in km $(mol)^{-1}$.

[c] Raman activity in Å$(amu)^{-1}$.

[d] The frequencies, IR intensities and Raman activities were calculated at level of theory of B3LYP/6-31G**.

[e] Brackets enclose the involved water molecules ordered according to their contribution. Labels between parentheses stand for vibrational mode combinations.

Please cite this article in press as: M.C. Bernini et al., Polyhedron (2011), doi:10.1016/j.poly.2011.10.030

adequate degree of deuterium substitution were employed to avoid ambiguity.

Several librational modes have been identified in the IR and Raman spectra. Supporting calculation shows that all of them involve all of the water molecules but sometimes a dominant role is played by a particular one. Two of these modes were confirmed by isotopic dilution experiments, the experimental $\nu H_2O/\nu HOD$ or $\nu H_2O/\nu D_2O$ ratios being in excellent agreement with the expected ones reported by Lutz [41]. The band at 790 cm^{-1} in the spectrum of the normal substance was identified as a water twisting mode. This band can be satisfactorily associated with that at 560 cm^{-1} in the IR spectrum of the partially deuterated compound which is originated in the same mode of the D_2O species. The corresponding isotopic ratio is 1.411 (expected value 1.415). On the other hand, a counterpart of a band at 537 cm^{-1} (H_2O) can be found at 446 cm^{-1} (HOD) in the IR spectrum upon partial deuteration. The calculated ratio of 1.204, near the 1.21 expected for a rocking mode, allow us to assign this signal to such vibration. Calculation also predicts a band at 569 cm^{-1} coming from the W3 rocking mode, with some contribution from the W2 rocking mode.

Finally, the band at 1247 cm^{-1} deserves a comment. This band clearly disappears with early dehydration and deuteration of water molecules, but it is absent in the theoretical IR spectrum calculated with the simplified model previously described. These facts could indicate that such a band is related to some kind of complex vibration of the water clusters that cannot be associated with any normal vibration because of its position. At the same time the band disappears during dehydration, a very weak shoulder near that position experiencing a strong activation. Taking into account the HB interactions that link methylene groups to W4 water molecules (see Table 3), a less restricted vibration for those groups, the activation and shifting of the mentioned band to a lower frequency could be attributed to release of W4 water molecule.

4. Conclusions

In the present work, we explore a MOF with enclathrated water molecules from a new perspective that consists in a deeper examination of the solvent structure in the solid state.

A strong influence of the MOF lattice through the stabilization micropore effect on the geometry of the water clusters is evidenced for the distorted chair-like conformation exhibited by A and B water hexamers. In turn, the development of the tape so modeled by the MOF environment, with several different anchoring points to the host lattice, has a crucial structural role that favors a suitable packing of the layers, stabilizes the 3D arrangement and makes evident its Templating For Guest function.

A complete and reliable assignment of the IR-Raman spectra of the infinite tape of water hexamers present in $[Er_2(C_4H_4O_4)_3(H_2O)_4]\cdot 6H_2O$ is reported. Theoretical calculations of the vibrational modes in a simplify model of the water tapes and isotopic dilution experiments support the assignment of the observed spectra, resulting in a useful combination of tools in the structural characterization of water substructures.

The results reported here could be extended to other crystalline environments containing water clusters as well as to detect and characterize water substructures in those cases where detailed structural information is not available.

Acknowledgments

The authors thank to Consejo Nacional de Investigaciones Científicas y Técnicas (CONICET: PIP 2008-01360, 2010-0985), Agencia Nacional de Promoción Científica y Tecnológica (PICT 03041, PICT 02315, PME06-2804), CSIC, Spain, Universidad Nacional de La Plata (UNLP), Universidad Nacional de San Luis (UNSL), Republica Argentina for financial support. G.P., A.F., G.A.E., and G.E.N. are members of the CONICET. M.C.B. acknowledges a CONICET fellowship.

Appendix A. Supplementary data

CCDC 805692 contains the supplementary crystallographic data for $[Er_2(C_4H_4O_4)_3(H_2O)_4]\cdot 6H_2O$. These data can be obtained free of charge via http://www.ccdc.cam.ac.uk/conts/retrieving.html, or from the Cambridge Crystallographic Data Centre, 12 Union Road, Cambridge CB2 1EZ, UK; fax: (+44) 1223-336-033; or e-mail: deposit@ccdc.cam.ac.uk. Supplementary data associated with this article can be found, in the online version, at doi:10.1016/j.poly.2011.10.030.

References

[1] L.J. Barbour, G.W. Orr, J.L. Atwood, Nature 393 (1998) 671.
[2] S.K. Ghosh, P.K. Bhadarwaj, Inorg. Chem. 42 (2003) 8250.
[3] Ch. Duan, M. Wei, D. Guo, Ch. He, Q. Meng, J. Am. Chem. Soc. 132 (2010) 3321.
[4] R. Ludwig, Phys. Chem. Chem. Phys. 4 (2002) 5481.
[5] (a) C.J. Tsai, K.D. Jordan, Chem. Phys. Lett. 213 (1993) 181;
(b) K. Kim, K.D. Jordan, T.S. Zwier, J. Am. Chem. Soc. 116 (1994) 11568.
[6] E.E. Dahlke, R.M. Olson, H.R. Leverentz, D.G. Truhlar, J. Phys. Chem. A 112 (2008) 3976.
[7] (a) R. Custelcean, C. Afloroaei, M. Vlassa, M. Polverejan, Angew. Chem., Int. Ed. 39 (2000) 3094;
(b) C. Foces-Foces, F. Hernández Cano, M. Martínez-Ripoll, R. Faure, C. Roussel, R.M. Claramunt, C. López, D. Sanz, J. Elguero, Tetrahedron: Asymmetry 1 (1990) 65.
[8] L. Infantes, S. Motherwell, CrystEngComm 4 (2002) 454.
[9] A. Michaelides, S. Skoulika, E.G. Bakalbassis, J. Mronzinski, Cryst. Growth Des. 3/4 (2003) 487.
[10] M. Mascal, L. Infantes, J. Chisholm, Angew. Chem., Int. Ed. 45 (1) (2006) 32.
[11] X.M. Zhang, R.Q. Fang, H.S. Wu, Cryst. Growth Des. 5/4 (2005) 1335.
[12] J.F. Song, J. Lu, J. Chen, Y.B. Liu, R.S. Zhou, X.Y. Xu, J.Q. Xu, Inorg. Chem. Commun. 9 (2006) 1079.
[13] A.T. Çolak, O.Z. YeŞilel, O. Büyükgüngör, Polyhedron 29/10 (2010) 2127.
[14] B.-Q. Ma, H.-L. Sun, S. Gao, Eur. J. Inorg. Chem. (2005) 3902.
[15] J. Yang, J.-F. Ma, Y.-Y. Liu, J.-C. Ma, H.-Q. Jia, N.-H. Hu, Eur. J. Inorg. Chem. (2006) 1208.
[16] Y.G. Sun, E.J. Gao, D.Z. Wei, Inorg. Chem. Commun. 10 (2007) 467.
[17] CAD4 Express Software, Enraf–Nonius, Delft, The Netherlands, 1994.
[18] K. Harms, S. Wocadlo, XCAD-4, Program for Processing CAD-4 Diffractometer Data, University of Marburg, Germany, 1995.
[19] G.M. Sheldrick, SHELXS86, Program for Crystal Structure Solution, Institut für Anorganische Chemie der Universität, Tammannstrasse 4, Göttingen, Germany, 1986.
[20] G.M. Sheldrick, SHELXL93, Program for the Refinement of Crystal Structures, University of Göttingen, Göttingen, Germany, 1993.
[21] M. Nardelli, J. Appl. Crystallogr. 32 (1999) 563.
[22] A.L. Spek, Acta Crystallogr., Sect. A 46 (1990) C34.
[23] PARST: M.J. Nardelli, Appl. Crystallogr. 28 (1995) 659.
[24] M.N. Burnett, C.K. Johnson, ORTEP-III Report ORNL-6895, Oak Ridge National Laboratory, Oak Ridge, Tennessee, USA, 1996.
[25] M.J. Frisch, G.W. Trucks, H.B. Schlegel, G.E. Scuseria, M.A. Robb, J.R. Cheeseman, V.G. Zakrzewski, J.A. Montgomery Jr., R.E. Stratmann, J.C. Burant, S. Dapprich, J.M. Millam, A.D. Daniels, K.N. Kudin, M.C. Strain, O. Farkas, J. Tomasi, V. Barone, M. Cossi, R. Cammi, B. Mennucci, C. Pomelli, C. Adamo, S. Clifford, J. Ochterski, G.A. Petersson, P.Y. Ayala, Q. Cui, K. Morokuma, D.K. Malick, A.D. Rabuck, K. Raghavachari, J.B. Foresman, J. Cioslowski, J.V. Ortiz, A.G. Baboul, B.B. Stefanov, G. Liu, A. Liashenko, P. Piskorz, I. Komaromi, R. Gomperts, R.L. Martin, D.J. Fox, T. Keith, M.A. Al-Laham, C.Y. Peng, A. Nanayakkara, C. Gonzalez, M. Challacombe, P.M.W. Gill, B. Johnson, W. Chen, M.W. Wong, J.L. Andres, C. Gonzalez, M. Head-Gordon, E.S. Replogle, J.A. Pople, GAUSSIAN 98, Revision A.7, Gaussian, Inc., Pittsburgh, PA, 1998.
[26] M.J. Frisch, G.W. Trucks, H.B. Schlegel, G.E. Scuseria, M.A. Robb, J.R. Cheeseman, J.A. Montgomery Jr., T. Vreven, K.N. Kudin, J.C. Burant, J.M. Millam, S.S. Iyengar, J. Tomasi, V. Barone, B. Mennucci, M. Cossi, G. Scalmani, N. Rega, G.A. Petersson, H. Nakatsuji, M. Hada, M. Ehara, K. Toyota, R. Fukuda, J. Hasegawa, M. Ishida, T. Nakajima, Y. Honda, O. Kitao, H. Nakai, M. Klene, X. Li, J.E. Knox, H.P. Hratchian, J.B. Cross, C. Adamo, J. Jaramillo, R. Gomperts, R.E. Stratmann, O. Yazyev, A.J. Austin, R. Cammi, C. Pomelli, J.W. Ochterski, P.Y. Ayala, K. Morokuma, G.A. Voth, P. Salvador, J.J. Dannenberg, V.G. Zakrzewski, S. Dapprich, A.D. Daniels, M.C. Strain, O. Farkas, D.K. Malick, A.D. Rabuck, K. Raghavachari, J.B. Foresman, J.V. Ortiz, Q. Cui, A.G. Baboul, S. Clifford, J. Cioslowski, B.B. Stefanov, G. Liu, A. Liashenko, P. Piskorz, I. Komaromi, R.L.

Martin, D.J. Fox, T. Keith, M.A. Al-Laham, C.Y. Peng, A. Nanayakkara, M. Challacombe, P.M.W. Gill, B. Johnson, W. Chen, M.W. Wong, C. Gonzalez, J.A. Pople, GAUSSIAN 03, Revision B.01, Gaussian, Inc., Pittsburgh, PA, 2003.
[27] A.D. Becke, J. Chem. Phys. 98 (1993) 5648.
[28] C. Lee, W. Yang, R.G. Parr, Phys. Rev. B 37 (1988) 785.
[29] J. Sun, Y.Q. Zheng, J.L. Lin, Z. Kristallogr.: New Cryst. Struct. 219/2 (2004) 99.
[30] M.C. Bernini, E.V. Brusau, G.E. Narda, G. Echeverría, C.G. Pozzi, G. Punte, C.W. Lehmann, Eur. J. Inorg. Chem. 5 (2007) 684.
[31] A.K. Cheetham, C.N.R. Rao, R.K. Feller, Chem. Commun. 46 (2006) 4780.
[32] (a) V.A. Blatov, IUCr Compcomm Newsl. 7 (2006) 4;
(b) V.A. Blatov, L. Carlucci, G. Ciani, D.M. Proserpio, CrystEngComm 6 (2004) 377.
[33] D. Tanaka, S. Kitagawa, Chem. Mater. 20 (2008) 922.
[34] D. Eisenberg, W. Kauzmann, The Structure and Properties of Water, Oxford University Press, Oxford, UK, 1969.
[35] A.H. Narten, H.A. Levy, in: F. Franks (Ed.), Water: A Comprehensive Treatise, Plenum, New York, 1972.
[36] Q.G. Meng, S.T. Yan, G.Q. Kong, X.L. Yang, Ch.D. Wu, CrystEngComm 12 (2010) 688.
[37] M.C. Bernini, J.C. Garro, E.V. Brusau, G.E. Narda, E.L. Varetti, J. Mol. Struct. 888 (2008) 113.
[38] K. Nauta, R.E. Miller, Science 287 (2000) 293.
[39] B. Berglund, J. Lindgren, J. Tegenfeldt, J. Mol. Struct. 43 (1978) 169.
[40] M. Falk, Spectrochim. Acta 40A (1) (1984) 43.
[41] H.D. Lutz, Structure and Bonding, Springer-Verlag, Berlin, Heidelberg, 1988.